Romanian Reports in Physics, Vol. 64, No. 4, P. 1072–1084, 2012

IMPACTS OF WIND FARMS ON WEATHER RADAR DATA AND SPATIAL RAINFALL ESTIMATION*

S. BURCEA[1,2], A. DUMITRESCU[1,3]

[1]National Meteorological Administration, Sos. Bucuresti-Ploiesti no. 97, 013686, Bucharest, Romania, E-mail: sorin.burcea@meteoromania.ro; alexandru.dumitrescu@meteoromania.ro
[2] University of Bucharest, Faculty of Physics, Atomistilor Str., Magurele, Ilfov, Romania
[3] University of Bucharest, Faculty of Geography, Blvd. Nicolae Balcescu no. 1., 010041, Bucharest, Romania

Received July 20, 2011

Abstract. Lately, the use of wind farms in Romania to generate electricity is growing. Wind turbines cause contamination of weather radar signals that is under certain conditions difficult to distinguish from weather echoes. Areas of false reflectivities, mean radial velocity and spectrum width data may appear in base data displays. These artifacts can affect and confuse weather forecasters and other radar data users. Since data from weather radars are key components in the decision making process of issuing severe weather warnings and nowcasting forecasts, and numerical weather models assimilation, this paper documents and addresses some of the impacts of wind farms on radar data. The WSR–98D radar at Medgidia was chosen for this study. A combination of low-resolution radar products and high-resolution data was used to document the impacts. The data have been used to construct a climatology of wind farm echo observation and to develop a GIS-based mitigation algorithm. The results of the study highlight the potential impacts of the wind farm echoes and the performance of the correction algorithm. The operational implementation of the mitigation algorithm was proposed.

Key words: radar observations, wind farm, GIS, algorithm.

1. INTRODUCTION

The use of wind farms as an alternative energy source is continuously growing in Romania, resulting into one of the most dynamic wind market in Eastern Europe. According to the Wind turbines and Windfarms Database and World Wind Energy Report 2010, the installed capacity has grown from 14 MW in 2009 to 591 MW in 2010 (*i.e.*, more than 4000% growth). A wind farm can have over 100 turbines with blade-tip heights reaching 150 m above ground level (AGL). During next years, a continued growth in the number of wind farms is expected.

* Paper presented at the Annual Scientific Session of Faculty of Physics, University of Bucharest, June 17, 2011, Bucharest-Magurele, Romania.

Fig.1 shows the wind farm locations in Romania, as present in the wind farms database (available at http://www.thewindpower.net). One can observe a concentration of wind farms in the south eastern part of the country, adjacent to the Black Sea, where the major wind farms are installed. Fig. 1 also depicts a part of the coverage area (100 km) from the total operational area coverage (230 km) of the Medgidia WSR–98D weather radar system (RDMD).

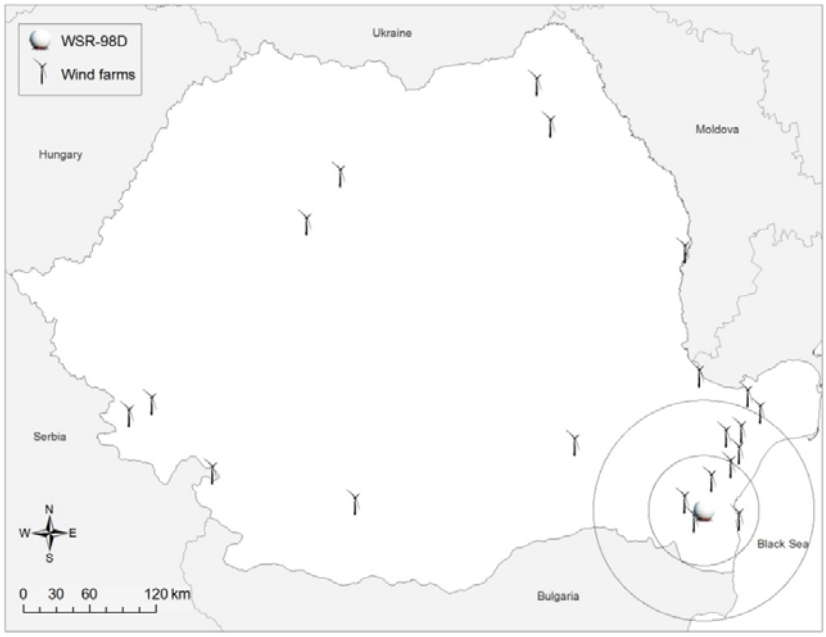

Fig. 1 – Locations of the wind farms and RDMD weather radar system in Romania. Range rings shown are 50 km apart**.**

While there are many positive aspects and benefits of the effort to expand wind energy, the negative impacts cannot be ignored. One such impact is the interference due to the presence of the wind farms on weather radar systems used to detect and monitor meteorological phenomena. Wind turbines are large structures, and combined with the rotation of the blades can result in the appearance of radar signatures similar with meteorological returns [2, 9, 11]. This type of interference is commonly known as wind turbine clutter (WTC). The detection of radar echoes caused by wind turbines are sometimes difficult to distinguish on a typical plan position indicator (PPI) display.

Previous research studies of the characteristics of WTC have been carried out to better understand their impact, characteristic signatures and mitigate their effects. Greving and Malkomes (2006, 2008) analyzed the effects of wind turbines on weather radars based on the radar cross section and recommended the use of mitigation schemes based on signal processing. Other studies characterized the

time variation of the WTC Doppler spectral signature. Isom *et al.* (2009) showed distinct flashes, Gallardo *et al.* (2008) showed a more complex Doppler spectrum evolution of the rotating blades. For air traffic control radar, mitigation techniques have been proposed or are in development. Techniques in development include track-inhibition algorithms [14], improving the range resolution of the radar to provide more uncontaminated resolution volumes between wind turbines, and adding telemetry to wind turbines to get real-time information about turbine angles relative to the radar or blade phase [4]. For weather radars, a few mitigation techniques have been proposed. One technique involves nonlinear filtering methods when in "spotlight" mode [10], while another technique involves the interpolation of spectral moment data over the wind farm using surrounding noncontaminated data [11].

The contaminated radar data induce errors in measurements of the weather parameters, and further can cause erroneous outputs of the radar algorithms. The quantitative precipitation estimation (QPE) is one algorithm that can be biased by wind farm interferences. In turn, biased algorithms can cause further problems to weather forecasters [15], false tornado or mesocyclone detections being also reported [3].

Data from the national Doppler weather radars network are a key component in the process of detection, monitoring and decision making of issuing severe weather warnings, and supporting the air traffic safety. Consequently, it is important to document the impacts of wind farms on weather radar data. This paper represents the first study on the impacts of wind farms on weather radars in Romania, and proposes a mitigation scheme of the impacts of wind farm returns on the data quality and nowcasting weather forecasts. The mitigation algorithm represents a GIS-based adjustment of the low level reflectivity measurements over the contaminated areas. Also, the paper provides background on the recent growth in the number of wind farms and examines some of their characteristics, and presents examples of impacts on radar products.

In the next section we describe the dataset and methodology used in the current study. Section 3 presents the results, interpretation and a proposed wind farm returns mitigation scheme. The last section contains the conclusions of the research.

2. DATA AND METHODOLOGY

Radar data are biased when the towers/blades are within radar beam line of sight (RLOS). The weather radar performs 360° scans of the atmosphere using different elevation angles of the antenna. The radar beam increases in height and in diameter as it moves away from the radar, with most of the emitted energy at the beam center height. There is reduced impact on the radar if the rotating blades are situated below the beam bottom (*i.e.*, points where the transmitted energy is 50% less than in the center of the beam). Thus, more impacts occur for wind farms that are very close to the radar site (*e.g.*, < 10 km).

One can observe the various locations of wind farms (operational or under construction) within the RLOS of 0.5° elevation beam of the RDMD (Fig.1). Currently, impacts on radar data are frequently observed from 3 wind farms located north east (NE), south west (SW), and north west (NW) of the RDMD. The NE wind farm is large (120 towers and turbines), producing a well distributed high reflectivity echo centered at approximately 50 km range (Fig. 2). The SW wind farm is not as large (~ 30 turbines), but it produces a distinctive radar echo approximately 20 km from radar (Fig. 2). Note that the terrain surface rises in the direction of the wind farms, allowing turbine blades to be within the beam line of sight at longer distances. Data displayed in Fig. 2 were sampled on 3 January 2011, at 0010 UTC (left) and 0347 UTC (right).

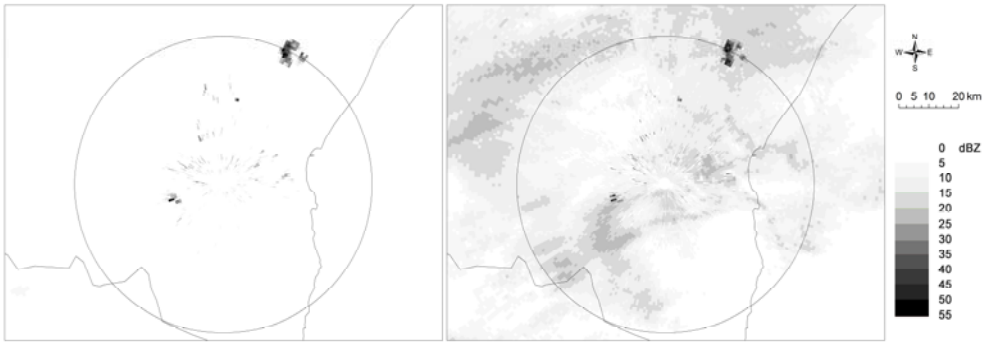

Fig. 2 – Reflectivity at 0.5° elevation angle showing the typical RDMD (left) clear air (no- precipitation) and (right) precipitation mode depiction of the NE and SW wind farms. Range rings shown are 50 km apart**.**

A much smaller farm is located NW, very close to the radar, at approximately 10 km away. Echoes produced by this wind farm are depicted in Fig. 2; the biases induced in the QPE algorithm are clearly seen on the precipitation accumulation radar products. No echo climatology was performed for this target, because echoes are detected virtually at every low elevation radar scan.

For the documentation of the impacts and for the development of a climatology of radar observations of the wind farms within RLOS, the Weather Surveillance Radar 98 Doppler (WSR–98D) operational at Medgidia (RDMD) was chosen for the study. The location of the radar unit is shown in Fig. 1. Base and derived radar product images covering the January–May 2011 period have been examined to document the impacts. High resolution digital data corresponding to the same period have been also used for the statistical analysis of the radar data and to construct the climatology of the wind farm echoes. Maps of frequency of detection and average reflectivity of the radar echoes were computed. The frequency of detection was defined as the percentage of the ratio of the times that a

radar bin exceeded the value of –25 dBZ to the total number of measurements over the respective bin. The average reflectivity for a radar bin was defined as the sum of reflectivity values divided by the total number of scans over the respective bin.

The analysis and mitigation of the spurious wind farm echoes were done using a Geographical Information System (GIS) based approach. The GIS geospatial techniques were proven to be viable in quantifying characteristics such as areal coverage and spatial patterns of weather events [1, 2, 13]. For the present study, we have been used the Inverse Distance Weighting (IDW) interpolation technique to correct the contaminated radar bins. Using IDW, the values of data bins in the neighborhood of each contaminated bin are averaged and the wind farm echoes are replaced with the corresponding values [12]. The closer a non-contaminated bin is to the bins erroneously detected and being estimated, the more influence, or weight, it has in the averaging process. In the current study, each contaminated bin was filled with the average of 8 neighborhood bins.

3. RESULTS AND INTERPRETATION

The results of the study highlight the influence of the wind farms detection on the quality of the radar measurements and precipitation estimates. The evaluation resulted in the development of a simple mitigation algorithm using a GIS-based approach. The algorithm significantly improves the data quality, providing the forecaster a better understanding of the detected weather phenomena. Radar precipitation estimates can also benefit from this approach, as the corrected reflectivity field is used to estimate the rainfall rate. Also, the most common impacts of wind farms were identified and documented.

3.1. CLIMATOLOGY OF WIND FARM ECHOES

Typical RDMD detected echoes in clear-air mode and precipitation mode (Fig. 2) reveal the appearance and spatial distribution of the wind farm returns. Observing the radar data for different weather events, it is very easy to see how wind farm returns might be mistaken for isolated thunderstorms in developing stage (Fig. 3) or for heavier storms within a widespread stratiform precipitation event (Fig. 2, right). The average maximum reflectivity at 0.5° elevation angle for both NE and SW wind farms is 40–50 dBZ. Radar echoes from both wind farms are seen at 0.5° elevation angle a vast majority of the time. One would expect that increasing the elevation of the antenna, the echoes would be more rarely seen. Wind farm echo observation at 1.5° elevation are still observed almost all the time for the SW wind farm, while the NE farm echoes occur more rare.

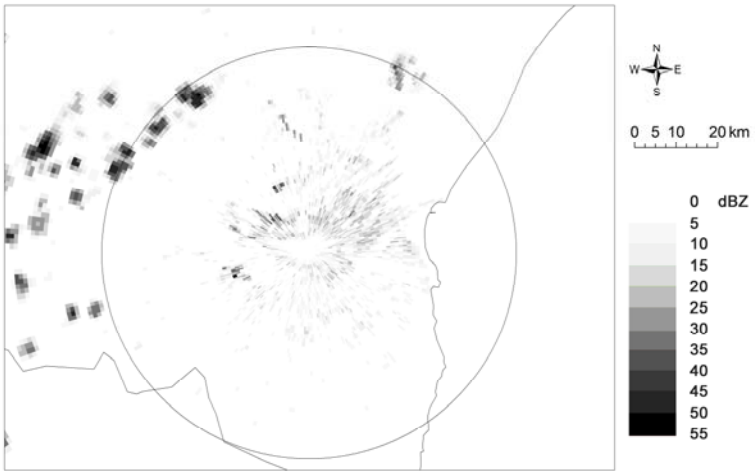

Fig. 3 – Reflectivity at 0.5° elevation angle showing newly-developing storms on 19 May 2011, 1052 UTC. The NE wind farm echoes can be mistaken with real storms. Range rings shown are 50 km apart.

Because wind farm returns are seen most of the time, but not all of the time, when observations show that both wind farms are within the 0.5° and 1.5° beams, a quantitative climatology of wind farm echoes was constructed. The methodology applied is similar with the one used by Burgess *et al.* (2008), consisting in observations of both wind farms made 8 times per day (every three hours). The period covered by the observations was 1 January–31 May 2011; a total of 150 days. The approximately 1100 observations included both precipitations and non-precipitation situations. Radar data loops were utilized to better understand weather phenomena evolution between observation times. The results (Fig. 4) indicate the diurnal and overall frequency of SW and NE wind farm returns greater than 15 dBZ.

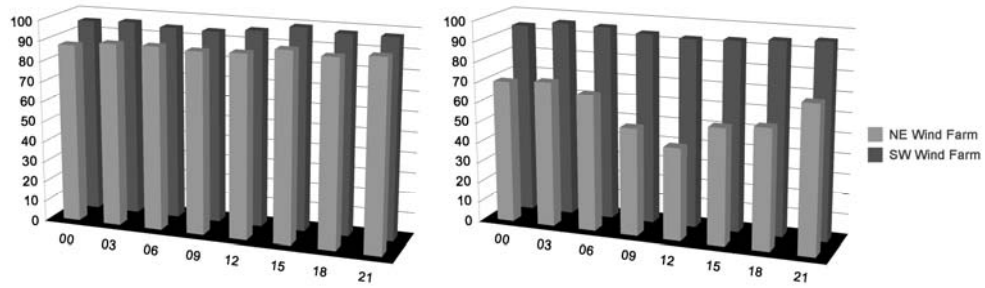

Fig. 4 – Five months climatology of radar echoes >15 dBZ for SW and NE wind farms at (left) 0.5° and (right) 1.5° elevation angles. Ordinate is percentage of observation, and abscissa is time (UTC) of observation.

At 0.5° elevation, echoes greater than 15 dBZ were observed 96% of the time for the SW wind farm, and 90% of the time for the NE wind farm. For this elevation, wind farm echoes did not displayed a noticeable diurnal trend. Burgess *et al.* (2008) found a diurnal trend of a major farm echoes located at approximately 40 km from the weather radar at Dodge City, Kansas, USA. In their case, wind farm echoes observation at and above 1.5° elevation was extremely rare. The current study shows a pronounced diurnal trend of the echoes when increasing the elevation angle to 1.5° (Fig. 4, right). The SW wind farm was still observed over 90% of the time, as the beam is not high enough to overshoot the wind turbines. Opposite, the NE wind farm exhibited a diurnal trend, being observed more frequently in the early morning and evening (70%), and less frequently in the afternoon (45%).

Special attention was given to those observation times when no echoes were observed. Additional study of the atmospheric soundings revealed that non-detection of the wind farms can result from two sources: sub-refraction of the radar beam (beam heights higher than under normal propagation conditions), and calm wind speeds. A sub-refraction example (Fig. 5) reveals the loss of echo from the NE wind farm after 1500 UTC, not returning until 2100 UTC, on 19 May 2011.

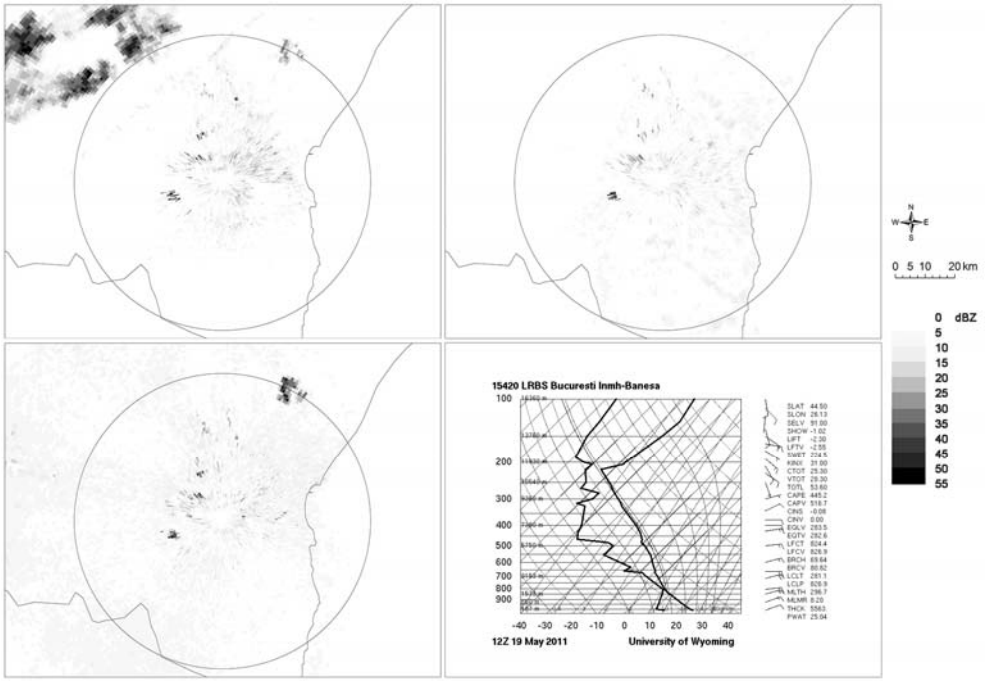

Fig. 5 – RDMD 0.5° reflectivity on 19 May 2011 showing the loss and reappareance of the NE wind farm echoes at 1458 UTC (up left), at 1804 UTC (up right), and at 2103 UTC (low left). Range rings shown are 50 km apart.

The 1200 UTC atmospheric sounding performed at Bucharest (Fig. 5, low right) features a low-level dry adiabatic lapse rate that, together with the afternoon warming and after dark cooling, produces the sub-refraction of the beam. When the winds are nearly calm so the blades are assumed not turning, the radar ground clutter suppression algorithm successfully removes the echoes from the wind farms.

3.2. ASSESSMENT OF THE RDMD RADAR MEASUREMENTS THROUGH REFLECTIVITY STATISTICS

A detailed analysis of the radar data quality and detection of the wind farm echoes has been done. The methodology consisted in computing the frequency of detection (FOD) and average reflectivity field (ARF) maps for the whole period (January–May 2011), using the high resolution data measured by the RDMD radar. The radar performs a volume scan of the atmosphere every 6 minutes. During this period, radar data availability was over 90%.

Frequency of detection maps at the 0.5° and 1.5° elevation angles are shown in Fig. 6 (left and right, respectively). FOD map at the 0.5° elevation (Fig. 6, left) highlight the areas where echoes from wind farms are detected. One can observe the high percentage of detection, over 90% of the time, for both SW and NE wind farms. The spatial annular pattern of the FOD reveals that no storm preferred tracks are present, the values decreasing from radar site to the end of coverage area. The speckle pattern of the high values around radar site is associated with the returns from the ground (clutter). FOD map at the 1.5° elevation (Fig. 6, right) is much more uniform, and the annular pattern is clearly visible, real measurements being better approximated. As the height of the beam is increasing with the distance from radar, low-altitude weather phenomena are overshooted (decreasing FOD). Still, echoes are detected from both wind farms, varying from 45–80 % of the time for the NE, and over 90 % of the time for SW.

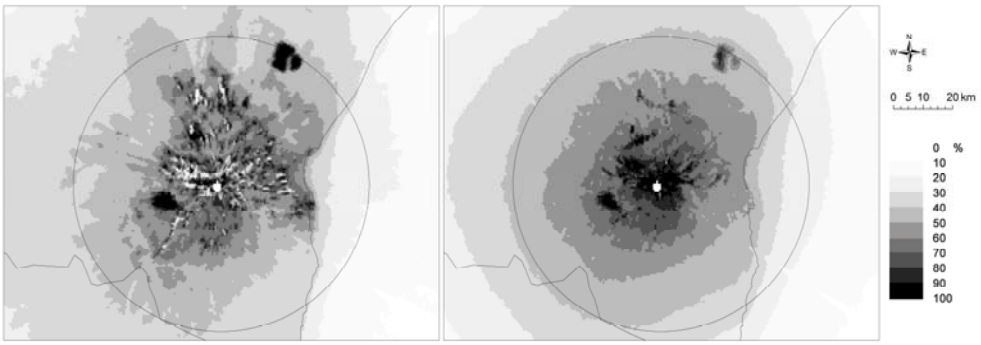

Fig. 6 – RDMD frequency of detection of echoes at (left) 0.5° and (right) 1.5° elevation angles, for the period January–May 2011. Range rings shown are 50 km apart.

In addition to the frequency of detection, the intensity of the radar echoes was investigated through the average radar reflectivity maps. Fig. 7 shows the ARF at the 0.5° and 1.5° elevation angles. At the 0.5° elevation (Fig. 7, left), one can easily identify the high reflectivity areas (40–50 dBZ) corresponding to the wind farm returns. The ARF field pattern at the 1.5° elevation (Fig. 7, right) is similar with the one at 0.5° for the areas where no wind farms are operational. Higher reflectivity values are observed only for the SW wind farm, but the areal extent is much smaller. The NE wind farm is rarely detected at this elevation.

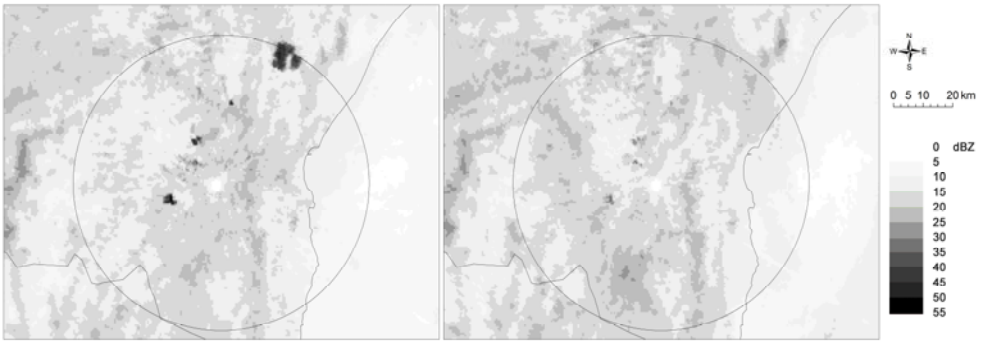

Fig. 7 – RDMD average reflectivity map at (left) 0.5° and (right) 1.5° elevation angles, for the period January–May 2011. Range rings shown are 50 km apart.

The maps are in agreement with the climatology results presented in the previous section, although the complete dataset analysis revealed much conclusive results. The 0.5° elevation climatology is consistent with the FOD and ARF maps, showing the highest rates of detection of both wind farms. At the 1.5° elevation angle, the climatology is in agreement with the results of the FOD map. The high temporal resolution dataset analysis shows that the NE wind farm is detected with a frequency between 50 and 80 %. While at the 0.5° the average value is 40–50 dBZ for the NE wind farm, at the 1.5° the value decreases around 20 dBZ.

Another feature depicted by the ARF maps is the reflectivity differences between echoes detected over the land compared with the ones detected over the sea. We speculate this is because the convection is most often initiated over the land than over the sea. Also, while examining the FOD map at 1.5° elevation, one can notice the shadow along the 126° radial as a result of the attenuation of the beam. This issues, together with the analysis of the Doppler radial velocity filed are not addressed in this paper.

3.3. MITIGATION OF THE WIND FARM ECHOES

As we showed in the previous sections, the RDMD data are contaminated with non-meteorological returns from ground (ground clutter, GC) and wind farms turbines (wind turbines clutter, WTC). As GC is mostly removed by the radar

algorithms, the WTC is difficult to remove because of the effect of losing valuable weather information. This can lead to wrong forecasts, as the intensity of the developing or existing storms can be underestimated. Also, the radar rainfall estimation is affected by the filtering of the data over the areas where wind farms are operational.

The RDMD radar rainfall estimation algorithm has the possibility to apply a number of sectorized areal data filters in order to reduce the impact of the contaminated echoes on the rainfall accumulation [5]. The exclusion areas are delimited between two azimuths, two radial distances, and with the possibility to specify the elevation angles between which the data exclusion to be done. This technique partially mitigates the erroneous accumulation estimates but produces regions of no estimate and loss of radar echo continuity.

During the streesful severe weather decision making and warning operations, the reflectivity field maps are the key component of the nowcasting forecaster main activity. Although the forecaster can get used with the areas and patterns of wind farms, it is possible that the radar data can be wrong interpreted. Also, the rainfall estimates algotithm can experince contamination with echoes that does not relfect the real situations, causing usually an overestimation of the rainfall at the ground.

For the improvement of the data quality, rainfall estimates and mitigation of the wind farm returns, a correction method is proposed. The methodology uses a GIS-based aproach, and performs the interpolation of the data over the areas of contaminated radar bins using the IDW interpolation technique.

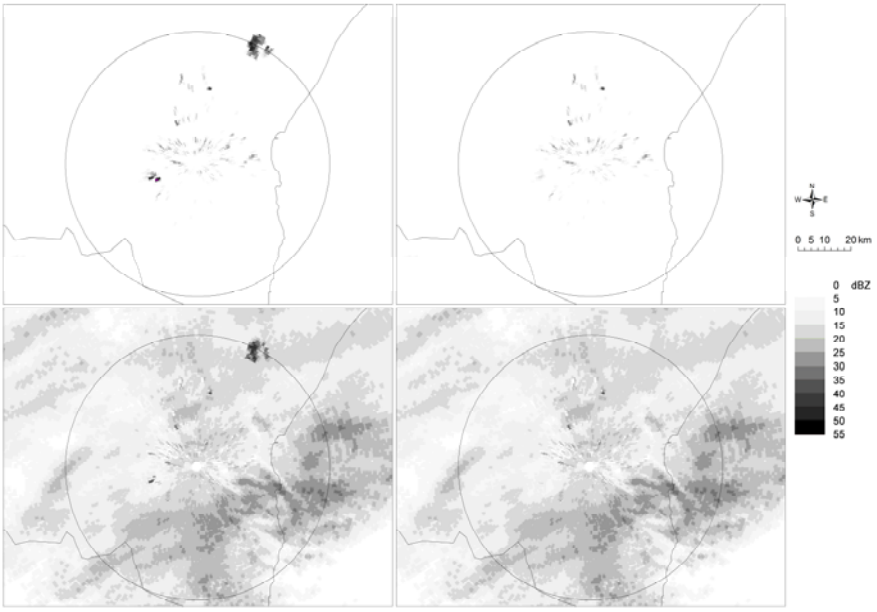

Fig. 8 – Results of the algorithm of mitigation of wind farm echoes. Times of observation are from 3 January 2011, at 0010 UTC (up) and 0347 UTC (down). Range rings shown are 50 km apart.

Fig. 8 (up) illustrates the outputs of the method for the case when no precipitation is detected within the radar coverage area. The NE wind farm echoes are completely removed (Fig. 8, up right), while the SW echoes are corrected. The algorithm performs well also in the case when weather echoes are detected (Fig. 8, down), with the corrected reflectivity field (Fig. 8, down right) reflecting a better approximation of the weather event. This simple algorithm can be very useful also for the correction of the rainfall estimates, as the lowest elevation angle is used for the rainfall estimation. The outputs of the algorithm are available imediatelly after the radar scan, so the method can be implemented as an operational tool.

4. SUMMARY AND CONCLUDING REMARKS

The study focuses on the assessment of the Medgidia WSR–98D radar wind farms detection, the mitigation of the effects on the data quality, and improvement of the rainfall estimates. Climatology of wind farms echoes was constructed to reflect the detection of the wind farm echoes. Using a GIS-based approach, frequency of detection and average reflectivity maps were computed to evaluate the impact of the wind farm returns on the radar measurements. Also, the impacts were documented and a mitigation scheme has been proposed.

The study was focused on the reflectivity data only. Future work is required on the velocity measurements issues caused by the wind farms returns. The algorithms that use as input the velocity data can produce errors in estimating different severe weather signatures (*e.g.*, mesocyclone, tornado vortex signature).

The most common impact of the wind farms is judged to be false storm identification. Examples in Fig. 2 (right) indicate the possibility that wind turbines echoes can easily be mistaken with stronger precipitation areas embedded within widespread events or with newly-developing storms (Fig. 3). Therefore, it is possible that the forecaster can issue a bad warning, evaluating erroneously the situation. For helping the forecaster and for minimizing the impacts of the wind farm returns, a mitigation scheme was proposed. The radar data are converted into GIS-ready file format and an adjusted output is computed by applying a geospatial interpolation method on the measured reflectivity field.

In the following the emphasized results are presented.

The RDMD data is biased by the returns from the wind farm echoes operational within the coverage area.

The echoes climatology at the 0.5° revealed that both SW and NE wind farms are detected over 90 % of the measuring time.

At the 1.5° elevation, the climatology shows that the closer wind farm (SW) is still detected with high frequency (> 90%), while the further situated wind farm (NE) presents a diurnal trend being less frequently detected in the afternoon.

The detailed analysis implying the computation of the high temporal resolution maps is in good agreement with the climatology constructed from observations made every 3 hours.

The average reflectivity maps reveals the strong returns from the wind farms, echoes that clearly biases the radar measurements and radar rainfall estimates.

The simple processing and mitigation algorithm can be implemented as an operational tool, as the computing is done automatically and the output is available very fast after the radar products are generated. The adjusted low level reflectivity field can be used for computing the rainfall rate over the area covered by radar, therefore improving the rain accumulation product.

The wind farm associated errors that occur both in clear air and precipitation mode represents a challenging research subject.

REFERENCES

1. J. B. Basara, D. Mitchell, D. R. Cheresnick, B. G. Illston, *An analysis of severe hail swaths in the Southern Plains of the United States*, Transactions in GIS, **11**, *4*, 531–554 (2007).
2. J. Billet, M. DeLisi, B. G. Smith, C. Gates, *Use of regression techniques to predict hail size and the probability of large hail*, Wea. Forecasting, **12**, *1*, 154–164 (1997).
3. D. W. Burgess, T. D. Crum, R. J. Vogt, *Impacts of wind farms on WSR-88D radars*, Preprints, 4th Int. Conf. on Interactive Information Processing Systems (IIPS) for Meteorology, Oceanography, and Hydrology, New Orleans, LA, Amer. Meteor. Soc., 6B.3, 2008 (Available online at http://ams.confex.com/ ams/pdfpapers/128810.pdf.).
4. J. M. Cornwall, *Mitigation of wind turbine effects on FAA and military radars*, Adapted from Jason Rep. JSR-07-126, MITRE Corporation, 2007.
5. R.A. Fulton, J. P. Breidenbach, D. J. Seo, D. A. Miller, T. O'Bannon, *The WSR-88D Rainfall Algorithm*. Wea. Forecasting, **13**, 377–395 (1998).
6. B. Gallardo, F. Perez, F. Aguado, *Characterization approach of wind turbine clutter in the Spanish Weather Radar Network*, Proc. Fifth European Conf. on Radar in Meteorology and Hydrology, Helsinki, Finland, European Meteorological Society, 9.8, 2008.
7. G. Greving, M. Malkomes, *On the concept of the radar cross section RCS of distorting objects like wind turbines for the weather radar*, Proc. Fourth European Conference on Radar in Meteorology and Hydrology, Barcelona, Spain, European Meteorological Society, 2006, P5.8.
8 G. Greving, M. Malkomes, *Weather radar and wind turbines – Theoretical and numerical analysis of the shadowing effects and mitigation concepts*, Proc. Fifth European Conf. on Radar in Meteorology and Hydrology, Helsinki, Finland, European Meteorological Society, 2008, P2.12.
9. K. Hood, S. Torres, R. Palmer, *Automatic Detection of Wind Turbine Clutter for Weather Radars*, J. Atmos. Oceanic Technol., **27**, 1868–1880 (2010).
10. B. M. Isom, *Characterization and mitigation of wind turbine clutter for the WSR-88D Network*, M.S. thesis, School of Electrical and Computer Engineering, University of Oklahoma, 2007.
11. B.M. Isom, and Coauthors, *Detailed Observations of Wind Turbine Clutter with Scanning Weather Radars*, J. Atmos. Oceanic Technol., **26**, 894–910, 2009.

12. K. Johnston, J. M. Ver-Hoef, K. Krivoruchko, N. Lucas, *Using ArcGIS Geostatistical Analyst*, ESRI. Redlands, 2001.
13. C.J. Matyas, *A Spatial Analysis of Radar Reflectivity Regions within Hurricane Charley (2004)*, J. Appl. Meteor. Climatol., **48**, 130–142 (2009).
14. J. Perry, A. Biss, *Wind farm clutter mitigation in air surveillance radar*, IEEE Aerosp. Electron. Syst. Mag., **22**, 35–40 (2007).
15. R. J. Vogt, J. Reed, T. Crum, J. T. Snow, R. D. Palmer, B. M. Isom, D. W. Burgess, *Impacts of wind farms on WSR-88D operations and policy considerations*, Preprints, 23rd Int. Conf. on Interactive Information Processing Systems (IIPS) for Meteorology, Oceanography, and Hydrology, San Antonio, TX, Amer. Meteor. Soc., 2007, 5B.7.